JOURNAL OF VIROLOGY, Sept. 1987, p. 2754–2763
0022-538X/87/092754-10$02.00/0

Vol. 61, No. 9

Generation of Altered Transcripts by Retroviral Insertion within the c-*myb* Gene in Two Murine Monocytic Leukemias

THOMAS J. GONDA,[1]* SUZANNE CORY,[2] PETER SOBIESZCZUK,[1] DOUGLAS HOLTZMAN,[1] AND JERRY M. ADAMS[2]

Ludwig Institute for Cancer Research, Melbourne Tumour Biology Branch,[1] and The Walter and Eliza Hall Institute of Medical Research, Royal Melbourne Hospital,[2] Victoria 3050, Australia

Received 16 December 1986/Accepted 19 May 1987

Two murine monocytic leukemia cell lines, WEHI-265 and WEHI-274, were found to carry a rearranged c-*myb* gene. The rearrangements are due to insertion of a deleted Moloney murine leukemia virus (Mo-MLV) provirus in the 5′ region of the c-*myb* gene and thus are similar to rearrangements in the ABPL tumors (G. L. C. Shen-Ong, M. Potter, J. F. Mushinski, S. Lavu, and E. P. Reddy, Science 226:1077–1080, 1984). In each cell line, the retroviral insertion has induced high levels of two aberrant RNA species, which, as in the ABPL tumors (G. L. C. Shen-Ong, H. C. Morse, M. Potter, and J. F. Mushinski, Mol. Cell. Biol. 6:380–392, 1986), contain both viral (Mo-MLV) and cellular (*myb*) sequences. Both species lack the sequences encoding the amino terminus of the c-*myb* protein and thus could encode a protein which, like the v-*myb* gene products (and the predicted ABPL *myb* proteins), is truncated at the amino terminus. We have found that the larger (5.3 kilobase [kb]) and more abundant of the tumor-specific *myb* RNAs was predominantly nuclear, while the smaller species (3.9 kb) was cytoplasmic. Furthermore, our data imply that the 3.9-kb RNA was derived from the 5.3-kb RNA by an additional splice which utilized a cryptic splice acceptor site within the viral *gag* sequences. On the basis of subcellular distribution and predicted translational potential, we conclude that the 3.9-kb RNA is probably the mRNA which encodes a truncated *myb* protein. We also show that, due to different insertion points in W265 and W274, the W274 *myb* RNAs contained sequences from a c-*myb* exon upstream of the exons represented in the W265 (and ABPL) RNAs. The significance of our findings with regard to transformation by *myb* in these tumors is discussed.

Transduction of coding sequences from the c-*myb* proto-oncogene of chickens has generated the acute leukemia viruses AMV and E26 (40), which transform cells of the monocytic lineage (3, 28). Comparison of the viral *myb* (v-*myb*) nucleotide sequences (19, 31, 41) with those of the murine (1, 15) and avian (39) c-*myb* genes has revealed that the v-*myb* genes lack coding sequences from both the 5′ and 3′ ends of c-*myb*. Thus, it has been suggested that truncation at the amino and/or carboxy terminus of the c-*myb* protein may be necessary or even sufficient to generate an oncogenic protein. This notion is supported by the identification of hematopoietic tumors in which retroviruses have inserted into the c-*myb* gene, in a manner predicted to lead to the synthesis of *myb* proteins truncated at either the amino (45) or carboxy terminus (45, 53).

The present report is concerned with two retrovirus-induced murine myeloid tumor cell lines, which we show are like the ABPL tumors (30, 46) in that they bear retroviral insertions in the 5′ region of c-*myb*. These lines, WEHI-265 and WEHI-274, clearly represent the monocytic lineage (50, 51), as do the ABPLs (45), although in earlier reports the ABPL tumors were described as lymphoid (30). In each case the retroviral insertions have induced the synthesis of aberrant *myb* transcripts which are expressed at high levels. Shen-Ong et al. (45) have recently reported that both Moloney murine leukemia virus (Mo-MLV) and *myb* sequences are present in the ABPL transcripts, suggesting that these transcripts are generated by a "promoter insertion" mechanism. Furthermore, their data imply that the fusion of viral and cellular RNA sequences (which involves RNA splicing from a "cryptic" donor site in the viral *gag* gene) occurred at the same position within c-*myb* that marks the 5′ boundary of the v-*myb*-related sequences. Thus, a protein translated from such an RNA species would resemble the v-*myb* proteins in lacking the same amino-terminal portion of the c-*myb* gene product.

Here, we characterize the two major *myb* RNA species in W265 and W274 and show that they lack sequences which encode the amino-terminal region of the c-*myb* protein. Like the RNAs of the ABPL tumors, both transcripts appear to be generated by initiation within the viral long terminal repeat (LTR) and splicing from a cryptic donor site in the viral *gag* gene to an acceptor site in c-*myb*. We found that the larger and more abundant species was predominantly nuclear, while the smaller species was cytoplasmic. Furthermore, we found that the smaller RNA species was generated by an additional splice within the viral sequences and suggest that this species is the mRNA encoding a truncated c-*myb* protein. In addition, we show that due to different insertion points in the two cell lines, the W274 *myb* RNAs contained sequences from a c-*myb* exon upstream of those exons represented in the W265 (and ABPL) RNAs. The presence and nature of the rearrangements in W265 and W274 have a number of interesting implications for our understanding of transformation by *myb*.

MATERIALS AND METHODS

Cells. The monocytic leukemia cell lines W265 and W274 were derived from tumors induced in BALB/c mice by infection with Abelson murine leukemia virus (Ab-MLV) pseudotyped with Mo-MLV (N. Warner, personal communication). The myeloid characteristics of these cell lines have been described previously (50, 51). W274.25 is a subclone of W274 isolated from an early passage of the original tumor

* Corresponding author.

and was provided by K. Leslie and J. Schrader (Walter and Eliza Hall Institute, Melbourne). The thymoma cell line RB22 (5) is nonproductively infected with Ab-MLV and was provided by W. Cook (Ludwig Institute, Melboune). Cells were maintained in Dulbecco modified Eagle medium containing 10% fetal calf serum.

Cloned DNAs and probes. The murine c-*myb* cDNA clones MM49 and MM46 have been described (15). Murine genomic c-*myb* clones covering the 5′ region of the gene were isolated by standard procedures (26) with the 0.7-kilobase (kb) *Eco*RI fragment of MM49 to probe BALB/c genomic libraries. These clones were analyzed by restriction mapping and hybridization to oligonucleotide probes corresponding to various parts of the c-*myb* sequence, including those described below. The c-*myc* intron probe was the 0.8-kb *Bgl*II-*Sac*I fragment from intron 1 of the murine c-*myc* gene and the Mo-MLV LTR probe was a 0.38-kb U3-specific fragment generated by digestion of cloned Ab-MLV proviral DNA with *Bam*HI and *Xba*I (48).

Oligonucleotide probes. Oligonucleotide probes complementary to the following sequences were synthesized with an Applied Biosystems model 380A DNA synthesizer. The sequence numbers referred to are those given (15) for the c-*myb* cDNA and from Shinnick et al. (47) for Mo-MLV. In each case, the probe sequence was complementary to the following sequences. (i) c-*myb* probes: exon 1, nucleotides 1 to 25; exon 2, nucleotides 87 to 109; exon 3, nucleotides 211 to 231; exon 4, nucleotides 262 to 282. (ii) Mo-MLV probes: U5, nucleotides 71 to 120; U3, nucleotides 8168 to 8217; *gag*, nucleotides 1361 to 1400. (iii) Splice-bridging probes: SO1, Mo-MLV nucleotides 194 to 205 and 1363 to 1374; SO2, Mo-MLV nucleotides 1585 to 1596 and c-*myb* nucleotides 177 to 188; SO3, Mo-MLV nucleotides 1585 to 1596 and c-*myb* nucleotides 250 to 261.

Cloned DNA fragments were radiolabeled by nick translation in the presence of [α-^{32}P]dATP. Oligonucleotides were labeled with T4 polynucleotide kinase and [γ-^{32}P]ATP. Reaction mixtures consisted of 13 to 16 pmol of oligonucleotide, 55 μCi of [γ-^{32}P]ATP (2,000 Ci/mmol), and 2 to 3 U of T4 kinase in 20 μl of 66 mM Tris, pH 7.6, 6.6 mM $MgCl_2$, and 5 mM dithiothreitol. After 30 min at 37°C, the reaction was terminated by adding sodium dodecyl sulfate (SDS) to 0.5% and EDTA to 10 mM and heating at 65°C for 5 min. Labeled oligonucleotides were collected by precipitation with 3 volumes of ethanol after adding ammonium acetate to 2 M and 20 μg of carrier DNA. This procedure removed the bulk of the unincorporated label.

Preparation and analysis of RNA. Total cellular polyadenylated [poly(A)$^+$] RNA was isolated by proteinase K-SDS treatment of cells followed by oligo(dT)-cellulose chromatography as described (16). Nuclear and cytoplasmic RNAs were prepared by a modification of published procedures (12, 26). Essentially, nuclear and cytoplasmic fractions were prepared by lysis in Nonidet P-40 and digested with proteinase K-SDS as described (26) except that (i) the nuclear pellet was disrupted by high-speed homogenization at the start of the proteinase K digestion to shear high-molecular-weight DNA and (ii) RNase inhibitors were omitted in most cases. Following proteinase K digestion, poly(A)$^+$ RNA was isolated directly from each fraction by absorption onto oligo(dT)-cellulose as described for the isolation of total poly(A)$^+$ RNA (16). The RNAs (3 μg per lane) were fractionated by formaldehyde-agarose gel electrophoresis and transferred to nitrocellulose filters for subsequent hybridization following procedures described elsewhere (16). RNA sizes were determined by using Mo-MLV and Ab-MLV viral RNAs as internal standards; their sizes were deduced from their DNA sequences (38, 47).

Hybridization conditions for RNA analysis. Hybridizations to nick-translated probes were carried out for 16 to 20 h at 42°C in buffer containing 50% formamide, 5× SSC (1× SSC is 0.15 M NaCl plus 0.015 M sodium citrate), 0.1% Ficoll, 0.1% bovine serum albumin, 0.1% polyvinylpyrrolidone, 100 μg of denatured salmon sperm DNA per ml, 2 mM EDTA, 0.1% SDS, and 10 mM HEPES (*N*-2-hydroxyethylpiperazine-*N*′-2-ethanesulfonic acid, pH 7.0). Usually 3×10^6 to 4×10^6 cpm of probe (specific activity, 1×10^8 to 4×10^8 cpm/μg) was added per ml. Filters were washed in 0.1% SDS–0.1× SSC at 50°C for several hours.

Hybridizations to the shorter (20 to 25 base) oligonucleotide probes were carried out in a solution containing 6× SSC, 0.1% Ficoll, 0.1% bovine serum albumin, 0.1% polyvinylpyrrolidone, 100 μg of denatured salmon sperm DNA per ml, 0.1% SDS, 2 mM EDTA, and 2 mM sodium PP_i. Usually 5 to 10 ng of labeled oligonucleotide was added per ml. Hybridizations to the shorter oligonucleotides were performed at 10 to 20°C below the estimated melting temperature for the hybrid; this was derived from the approximation: T_m = 4(no. of G+C residues) + 2(no. of A+T residues) (27). Filters were washed in 6× SSC–0.1% SDS at the same temperature. The longer (40 or 50 base) oligonucleotides were hybridized at 37°C in the formamide buffer described above with the addition of 2 mM sodium PP_i, and filters were then washed at 50°C in 0.5× SSC–0.1% SDS.

RESULTS

c-*myb* rearrangements in murine hematopoietic cell lines. To investigate the possible involvement of c-*myb* in myeloid leukemia, we surveyed 17 murine hematopoietic cell lines for rearrangements and aberrant expression of the c-*myb* gene (Table 1). An *Eco*RI digest of genomic DNA from each line was probed with a murine c-*myb* cDNA clone, and in some cases RNA was also examined by Northern blotting (RNA blotting). Rearranged c-*myb* alleles (Fig. 1A) and abnormally sized *myb* transcripts (see below) were evident in two of the lines, W265 and W274, both of which were induced by the Ab-MLV/Mo-MLV complex (N. Warner, personal communication). None of the other 15 lines exhibited an aberrant c-*myb* *Eco*RI fragment, even though several were derived by retroviral infection. The RAW264.7 line (37) was of particular interest because, like W265 and W274, it did not carry a v-*abl* gene (Table 1), even though it was also derived from a tumor induced by the Ab-MLV/Mo-MLV complex.

During the course of this survey it became clear that the murine c-*myb* gene displayed polymorphism, as has previously been reported for the human c-*myb* gene (10). Tumors derived from DBA/2 or C57BL/6 × DBA/2 mice (e.g., P388D1 and 416B in Fig. 1C) exhibited a novel 6.4-kb *Eco*RI fragment and lacked the 3.4-kb fragment characteristic of BALB/c lines such as WEHI-3B, W265, W274, and J774 (Fig. 1A). Analysis of liver DNA from the different mouse strains (data not shown) confirmed our conclusion that C57BL/6 and DBA/2 mice carry the same allele and also demonstrated that, like BALB/c mice, A/J mice carry the other c-*myb* allele.

W265 and W274 contain retroviral insertions in c-*myb*. In both W265 and W274, hybridization to the 4.2-kb *Eco*RI fragment containing exons 3 to 5 was diminished and an additional band was seen at 8 kb (Fig. 1A; revealed by increased intensity in the case of W274). This observation

TABLE 1. Status of c-*myb* in murine hematopoietic cell lines

Cell line	Inducer	v-*abl*[a]	DNA[b]	RNA[c]	Reference(s)
Myelomonocytic					
WEHI-265	Ab-MLV (Mo-MLV)	−	R	R	50, 51
WEHI-274	Ab-MLV (Mo-MLV)	−	R	R	50, 51
416B	Friend MLV	−	N	N	8
WEHI-3B	Mineral oil	−	N	N	52
FDC-P1	Spontaneous	−	N	N	9
Raw 309 F1.1	Ab-MLV (Mo-MLV)	+	N	ND	37[d]
Macrophage					
RAW 309 Cr.1	Ab-MLV (Mo-MLV)	+	N	−	37
RAW 264.7	Ab-MLV (Mo-MLV)	−	N	−	37
WR 19M.1	Ab-MLV (Mo-MLV)	+	N	−	37
P388 D_1	Methylcholanthrene	−	N	ND	21
PU-5-1.8	Spontaneous	−	N	−	34
J774	Mineral oil	−	N	−	35
Mastocytoma					
HC.3	Spontaneous	−	N	ND	13
P-815X-2.1	Methylcholanthrene	−	N	ND	42
Mast cell					
WW	Spontaneous	−	N	ND	—[e]
R6-XE.4	Spontaneous	−	N	ND	43
Erythroleukemia (F4N)	Friend MLV	−	N	ND	7

[a] Presence (+) or absence (−) of v-*abl* sequences in the genome.
[b] Normal (N) or rearranged (R) configuration of c-*myb* sequences as determined by *Eco*RI digestion.
[c] Presence of normal-sized (N) or aberrant (R) c-*myb* transcripts or absence (−) of detectable c-*myb* RNA. ND, Not determined.
[d] RAW 309F1.1 was originally designated lymphoid (37) but appears instead to be myeloid as it is MAC-1 positive and lacks rearrangement of immunoglobulin loci or T cell γ or β loci (S. Cory, A. Harris, and W. Langdon, unpublished).
[e] —, J. W. Schrader and S. Schrader, unpublished data.

suggested that one c-*myb* allele in each line may have acquired an insert of approximately 4 kb within the 4.2-kb *Eco*RI fragment, which lies in the 5′ portion of the c-*myb* locus (see below). Furthermore, the inserted DNA was apparently related to Mo-MLV, since a probe specific for the Mo-MLV LTR hybridized to fragments in W265 and W274 DNA (arrow in Fig. 1B) that were indistinguishable in size from the altered c-*myb* fragments. Thus, the c-*myb* rearrangements in W265 and W274 appeared similar to those reported in the ABPL tumors (30, 46), in which deleted Mo-MLV proviruses are inserted within this same 4.2-kb c-*myb* *Eco*RI fragment. We estimate the sizes of the inserts in W265 and W274 to be 4.0 and 3.5 kb, respectively.

To aid further characterization of the c-*myb* rearrangements, we determined the structure of the 5′ region of the normal murine c-*myb* gene. This was achieved by isolating genomic clones encompassing this region and analyzing them by hybridization with a series of oligonucleotide probes representing sequences in the 5′ portion of the c-*myb* mRNA. The positions of exons 1, 2, and 3 were then localized precisely by nucleotide sequencing. Our data are essentially in agreement (see legend to Fig. 2) with other recently published structural analyses of the murine c-*myb* gene (1, 4, 24). The 12-kb region shown in Fig. 2 contains the start site(s) for *myb* transcription (8; unpublished data) and the first five exons of the c-*myb* gene. Exon 1 (designated UEIII in reference 24) contains the probable initiation codon for the c-*myb* protein (1, 14, 15). Sequences homologous to v-*myb* were present in exons 4 and 5 (VE1 and VE2 [45]) but not in exon 1, 2, or 3.

The sites of the retroviral insertions were deduced from the restriction map of the 5′ region of c-*myb* (Fig. 2) and the sizes of the rearranged fragments detected in W265 and W274 DNA by probes (a and b in Fig. 2) derived from the genomic clones. Hybridization of *Eco*RI digests with probe b confirmed that the insertions in both cell lines mapped within the 4.2-kb *Eco*RI fragment (Fig. 3A). The sizes of the *Pst*I fragments detected by probe a (Fig. 3B) were used to determine both the position and orientation of the inserts, since there is a *Pst*I site 1,014 base pairs (bp) from the 5′ end of the Mo-MLV provirus (47). These data were confirmed and refined by analysis of additional digests (with *Eco*RI plus *Pst*I, *Sac*I, and *Xba*I) with both probes (Fig. 3B). The restriction sites used for these analyses and the resultant localizations of the proviral inserts are shown in Fig. 2. The insert in W265 lay within a region about 200 bp upstream of exon 4, while that in W274 lay within a similar range near the 5′ boundary of exon 3. These positions are consistent with analyses of the *myb* RNAs in each cell line (see below). Furthermore, it can be seen that the inserts in both W265 and W274 had the same transcriptional orientation as c-*myb*, as did those in the ABPL tumors (46).

Two altered *myb* transcripts in W265 and W274. Since retroviral insertion in cellular genes often affects their transcription (reviewed in reference 32), we examined W265 and W274 for the presence of altered c-*myb* RNAs. For both cell lines, hybridization of poly(A)$^+$ RNA with a *myb* cDNA probe revealed an abundant 5.3-kb species and smaller amounts of a 3.9-kb species (Fig. 4A), neither of which appeared to be a normal c-*myb* transcript (see below). (Since W274 contained a large excess of the 5.3-kb RNA over the 3.9-kb species, the latter species was often not clearly discernable in whole-cell RNA preparations such as that shown in lane 2.) Furthermore, analysis of RNA from nuclear and cytoplasmic fractions of each cell line revealed that the 5.3-kb species was predominantly nuclear (Fig. 4A,

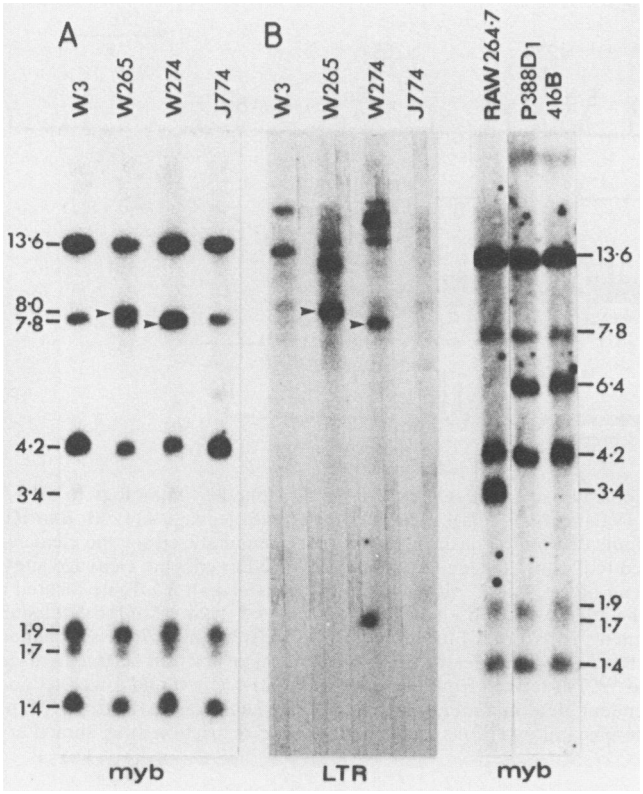

FIG. 1. Detection of c-*myb* rearrangements due to proviral insertion in W265 and W274. *Eco*RI-cut DNA from the indicated cell lines (Table 1) was analyzed by Southern blotting as described elsewhere (6). Hybridization was with (A) the murine c-*myb* cDNA clone MM49 (15) and (B) an LTR-specific probe (see Materials and Methods). The bands that comigrated with the additional fragments detected by the *myb* probe (A) are arrowed. (C) Polymorphism of c-*myb* between mouse strains. *Eco*RI digests were analyzed by hybridization to the MM46 c-*myb* cDNA clone (15). The RAW 264.7 tumor (37) arose in a BAB/14 mouse, P388D1 (21) in a DBA/2 mouse, and 416B (8) in a C57BL/6 × DBA/2 F_1 mouse. Note that the increased intensity of hybridization to the 3.4-kb (and 6.4-kb) fragments in panel C compared with panel A is due to the use of different (but overlapping) cDNA clones.

lanes 5 and 6), whereas the 3.9-kb RNA was found preferentially in the cytoplasm (Fig. 4A, lanes 3 and 4). This observation suggests that the 5.3-kb RNA may be a nuclear precursor of the 3.9-kb species. Moreover, at least some of the 5.3-kb RNA which was found in the cytoplasmic fraction resulted from its contamination with nuclear RNA (probably due to lysis of nuclei during the fractionation procedure), since unspliced c-*myc* precursor RNAs were also detectable in the cytoplasmic fractions (Fig. 4B). However, we cannot exclude the possibility that a small proportion of the 5.3-kb RNA was transported to the cytoplasm. The presence of some 3.9-kb RNA in the nucleus was not unexpected if the 3.9-kb species is a mature mRNA, as we suggest below.

Both the 3.9- and the 5.3-kb RNA species seen in W265 and W274 appeared to be aberrant c-*myb* transcripts. The 3.9-kb RNA did not comigrate precisely with either the major or minor normal c-*myb* transcript (see Fig. 5, 6, and 7), which we measured as 3.6 and 4.0 kb, respectively. Moreover, in contrast to the normal 3.6-kb and 4.0-kb c-*myb* RNAs in the thymoma cell line RB22 (Fig. 5, lane 1), neither the 5.3-kb nor the major 3.9-kb RNA species (Fig. 5, lanes 2 to 5) hybridized to oligonucleotide probes representing exon 1 or 2. Although these probes did detect a minor species of 3.8 kb (lanes 2 and 3), the latter species was of low abundance and distinct from the major 3.9-kb RNA. This is apparent from the low extent of hybridization of 3.8 to 3.9 kb RNA to the exon 1 and 2 probes compared with the exon 4 probe (Fig. 5, lanes 2 and 3), particularly when one takes into account the degree of hybridization of each probe to the normal 3.6-kb c-*myb* RNA (lane 1). We suspect that the 3.8-kb species may be transcribed from the unrearranged c-*myb* allele (possibly initiating at a position different from those which give rise to the usual 3.6- and 4.0-kb c-*myb* RNAs [1]). In any case, the hybridizations with the exon 1 and 2 probes revealed that the unrearranged c-*myb* alleles in W265 and W274 were transcribed at a low level, if at all.

A clear difference between the RNAs of W265 and W274 was revealed by hybridization to the exon 3 probe (Fig. 5). The major *myb* RNA species in W265 failed to react with this probe (lanes 2 and 4), while those in W274 (and of course RB22) hybridized strongly (lanes 3, 5, and 1). In contrast, the exon 4 probe labeled the 5.3-kb and 3.9-kb RNAs from both myeloid lines. The presence of exon 3 sequences in the *myb* transcripts of W274 but not W265 was consistent with the positions of the viral insertions in each line (Fig. 2) if the transcripts were generated by a viral promoter insertion mechanism (see below). Furthermore, the hybridization of W265 and W274 RNAs to the exon 4 probe (which represents sequences at the 5′ boundary of the v-*myb*-related region of c-*myb*), as well as to both the 5′ and 3′ *Eco*RI fragments of the cDNA clone MM49 (15) (Fig. 4 and 8, and data not shown), suggests that the aberrant *myb* transcripts contained all of the *myb* sequences homologous to the v-*myb* genes.

Viral sequences in the *myb* RNAs of W265 and W274. We next wished to determine whether the tumor-specific *myb* RNAs contained viral (i.e., Mo-MLV) sequences. Synthetic oligonucleotide probes were used for this purpose since they allow detection of an RNA containing only a small proportion of the relevant gene even in the presence of other RNAs containing a much greater proportion, a situation in which larger probes can give misleading results. As shown in Fig. 6, a probe representing the U5 region of the Mo-MLV LTR hybridized to a predominantly nuclear 5.3-kb RNA in both W265 and W274 (lanes 2 and 4), as well as to an unidentified 1.4-kb RNA in W274 (lane 3). The U5 probe also labeled the abundant 8.5-kb Mo-MLV genomic and 3.2-kb subgenomic viral transcripts in these cells (lanes 1 to 4) and the 5.3-kb Ab-MLV genomic transcript in RB22 (lane 5). Similarly, hybridization to a *gag* probe also revealed, in addition to the Mo-MLV genomic RNA, a predominantly nuclear 5.3-kb RNA in each cell line (lanes 2 and 4). In contrast, a probe representing the U3 region of the LTR did not detect a 5.3-kb RNA in either W265 or W274 (lanes 1 to 4), although, as expected, it did label the Mo-MLV RNAs in these cells and the Ab-MLV RNA (lane 5). Because the 5.3-kb RNAs detected with the *myb* probes (Fig. 4 and 5) and the *gag* and U5 probes (Fig. 6) not only comigrated precisely (data not shown) but showed the same subcellular distribution and relative levels in W265 and W274 (compare Fig. 5 and 6), we conclude that in each case we were detecting the same RNA species. Thus, the 5.3-kb RNAs of W265 and W274 contained *myb*, *gag*, and U5 sequences, as was also found for RNA from the ABPL tumors (45).

The data in Fig. 6 also indicated the origin of the proviral insertions within c-*myb*. Since the *gag* oligonucleotide represents sequences absent from Ab-MLV, as illustrated by its failure to hybridize to the Ab-MLV RNA in the RB22 cell

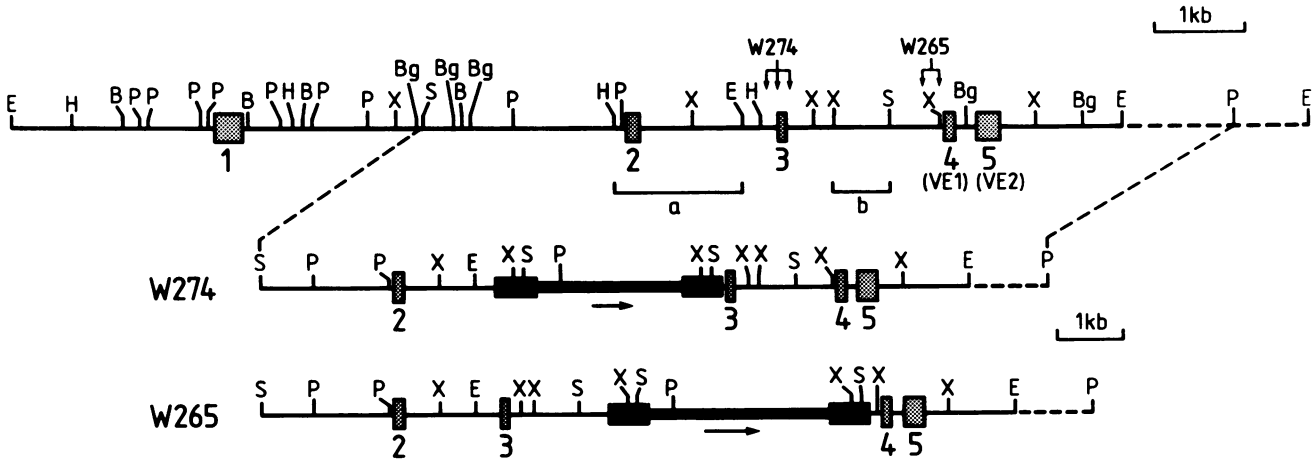

FIG. 2. (Top) Structure of the 5′ region of the murine c-*myb* gene. Stippled boxes represent exons 1 to 5, defined by homology to cDNA sequences; exons 4 and 5 correspond to the first two v-*myb*-related exons (VE1 and VE2 [45]). Restriction enzyme cleavage sites: B, *Bam*HI; Bg, *Bgl*II; E, *Eco*RI; H, *Hin*dIII; P, *Pst*I; S, *Sac*I; X, *Xba*I. The region indicated by the dashed line has not been analyzed for the cleavage sites of all of these enzymes. (This map differs from that of Lavu and Reddy [24] in the location of some restriction enzyme cleavage sites. With respect to their map we found [i] no *Xba*I site 600 bp from the 5′ end of the 8-kb *Eco*RI fragment, but instead an *Xba*I site located a similar distance from the 3′ end of this fragment; [ii] the *Xba*I site near the middle of the 8-kb *Eco*RI fragment is 5′ [not 3′] to the *Sac*I site; [iii] the third *Bam*HI site [~3 kb from the 5′ end of the 8-kb *Eco*RI fragment] is 3′ [not 5′] to the *Hin*dIII site; [iv] a third *Bgl*II site 400 bp 5′ to the *Bam*HI site 5 kb from the 5′ end of the 8-kb *Eco*RI fragment.) Bars a and b beneath the map represent restriction fragments used as probes. Also shown are the positions of proviral insertion in W265 and W274 (derived from the data of Fig. 3; see text and lower section of this figure); the range of positions calculated from several independent determinations is indicated in each case. (Bottom) Maps representing the corresponding regions in W265 and W274, including the proviral insertions (solid boxes). The restriction sites shown are those relevant to the mapping experiments of Fig. 1 and 3 (see text).

line (lane 5), hybridization of the 5.3-kb RNAs in W265 and W274 to the *gag* probe indicates that the proviral insertions must have come from Mo-MLV rather than Ab-MLV. This conclusion is consistent with the absence of v-*abl* sequences from W265 and W274 (Table 1).

The analyses shown in Fig. 6 did not clearly reveal hybridization of the 3.9-kb *myb* RNA in either W265 or W274 to any of the viral probes. Since this RNA may have been obscured by degradation products of the much more abundant Mo-MLV RNA, we examined a subline of W274 which lacks the normal Mo-MLV transcripts. This line, W274.25, has a c-*myb* rearrangement identical to that of the parental line (K. Leslie, personal communication), and hybridization with the c-*myb* exon 4 probe (Fig. 7) revealed the same nuclear and cytoplasmic RNA species (cf. Fig. 5). Hybridization with the *gag* and U5 probes clearly revealed that the 3.9-kb as well as the 5.3-kb species contained sequences from these regions of Mo-MLV. Although no

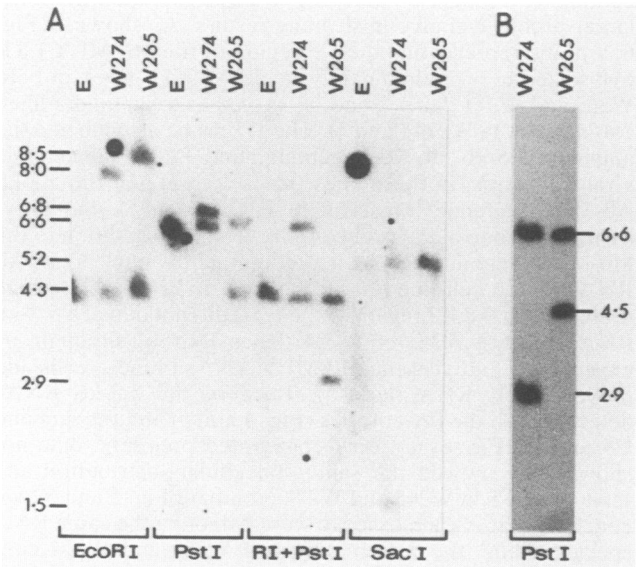

FIG. 3. Mapping of retroviral insertion sites within c-*myb* in W265 and W274. (A) DNAs from BALB/c mouse embryo (E), W274, and W265 were digested with the indicated restriction endonucleases and analyzed by Southern blotting with probe b (Fig. 2). (B) DNAs from W265 and W274 were digested with *Pst*I and analyzed by hybridization to probe a (Fig. 2).

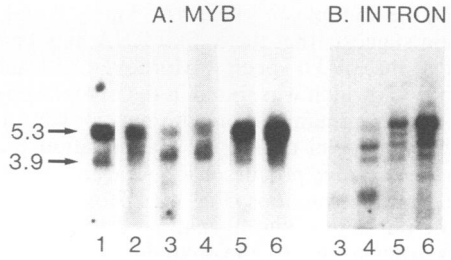

FIG. 4. Identification and subcellular distribution of poly(A)$^+$ c-*myb* transcripts in W265 and W274 by Northern blotting. The sizes of the major species (in kilobases) are indicated at left. The probes used were (A) c-*myb* cDNA and (B) c-*myc* intron. Lanes: 1, total cellular RNA from W265; 2, total cellular RNA from W274; 3, cytoplasmic RNA from W265; 4, cytoplasmic RNA from W274; 5, nuclear RNA from W265; 6, nuclear RNA from W274. The W265 lanes represent longer autoradiographic exposures than the corresponding W274 lanes in order to clearly illustrate the RNA species present in W265. The smallest species in panel B represents mature c-*myc* mRNA and was detected by contaminating exon sequences in the probe, while the remaining species are nuclear precursors.

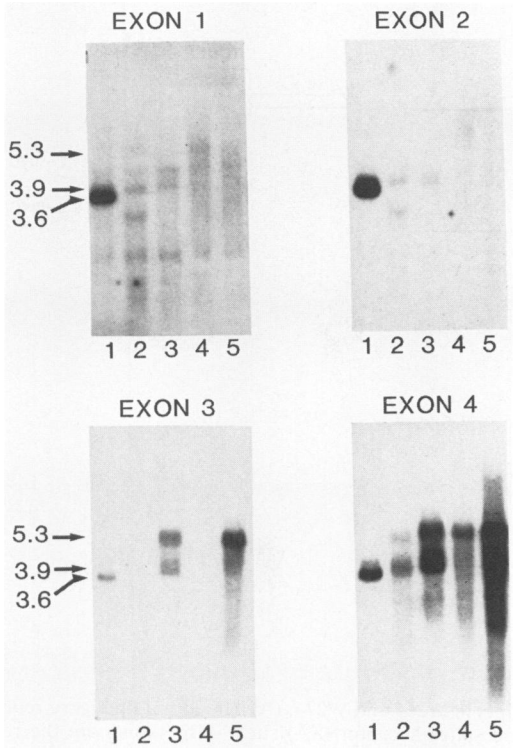

FIG. 5. Presence of c-*myb* exon sequences in normal and aberrant c-*myb* transcripts. Poly(A)$^+$ RNAs were analyzed by Northern blotting and hybridization to oligonucleotide probes representing c-*myb* exons 1 to 4 as indicated. Sizes of the major normal and aberrant *myb* transcripts (in kilobases) are indicated at the left. Lanes: 1, cytoplasmic RNA from the thymoma cell line RB22; 2, cytoplasmic RNA from W265; 3, cytoplasmic RNA from W274; 4, nuclear RNA from W265; 5, nuclear RNA from W274.

similar variant of W265 was available to complete this analysis, other data presented below show that the 3.9-kb from W265 RNA contained some *gag* sequences.

Surprisingly, we could not detect transcripts corresponding in size to the deleted proviruses in either line with any of the viral probes (Fig. 6 and 7). Clearly, transcription proceeds beyond the 3′ ends of these proviruses to generate the hybrid viral-*myb* RNAs; we can only conclude that for unknown reasons this readthrough is very efficient.

Splicing patterns of the tumor-specific *myb* RNAs. The presence of viral U5 and *gag* sequences in the *myb* RNAs of

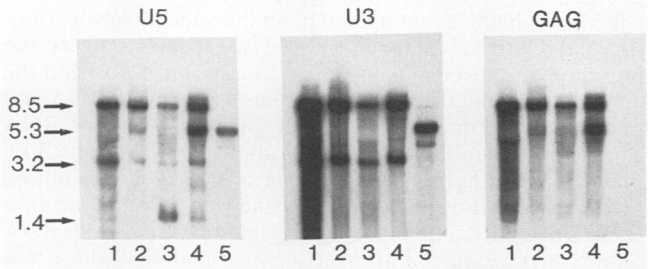

FIG. 6. Transcription of viral sequences in W265 and W274 analyzed by Northern blotting and hybridization to oligonucleotide probes representing the indicated retroviral sequences. Lanes: 1, cytoplasmic RNA from W265; 2, nuclear RNA from W265; 3, cytoplasmic RNA from W274; 4, nuclear RNA from W274; 5, cytoplasmic RNA from the thymoma cell line RB22. The sizes of the major RNA species (in kilobases) are indicated at left.

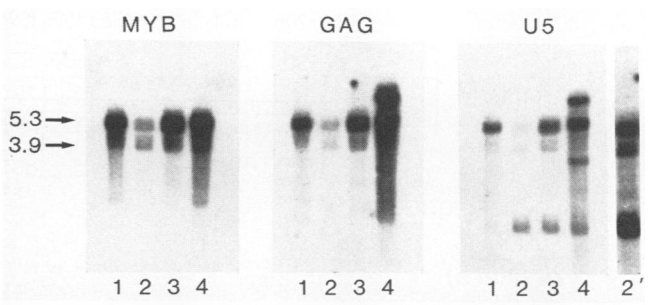

FIG. 7. Analysis of v-*myb* hybrid transcripts in the W274 variant W274.25 by Northern blotting. Lanes 1, 2, and 3, nuclear, cytoplasmic, and total RNAs, respectively, from W274.25; lanes 4, total RNA from the standard W274 line for comparison. Lane 2′ is a longer autoradiographic exposure of lane 2. Hybridization was to the c-*myb* exon 4 probe and to the U5 and *gag* probes, as indicated. Sizes (in kilobases) are shown at the left.

W265 and W274 can most readily be explained by RNA splicing, as suggested for the ABPL tumors (45). To establish this and to account for the two classes of *myb* RNA in these lines, we designed bridging oligonucleotide probes to detect the results of specific splicing events.

To test for specific *gag-myb* splices, we used 24-base oligonucleotides complementary to (i) the 12 nucleotides 5′ to the cryptic splice donor site within *gag* (at position 1596 of the Mo-MLV sequence) identified by Shen-Ong et al. (45) (SD_c in Fig. 8A) and (ii) the 12 nucleotides 3′ to the c-*myb* acceptor sites at the exon 3 or exon 4 boundary (oligonucleotides SO2 and SO3, Fig. 8A). Under the hybridization and washing conditions used, these probes should hybridize only to an RNA species in which the 24 nucleotides are contiguous, i.e., only if the predicted splicing event has occurred. Figure 8B shows that SO2 hybridized to RNA from W274 (lanes 3 and 4) and SO3 to RNA from W265 (lanes 1 and 2), exactly as predicted from the insertion mapping (Fig. 2 and 3) and by the RNA hybridization from the insertion mapping (Fig. 2 and 3) and by the RNA hybridization data of Fig. 5. Moreover, the same *gag-myb* splices occurred in both the 5.3-kb and 3.9-kb RNAs. We cannot fully explain the weak hybridization of SO3 to the larger RNA species in W274 (Fig. 8B, lanes 3 and 4). These bands may be due to partial homology between SO3 and the W274 RNAs or may indicate that a small proportion of the *myb* RNAs in W274 resulted from splicing to exon 4. In any case, the 3.9-kb RNA which we believe to be the functional *myb* mRNA was not detected by SO3 (lane 3), so splicing to exon 4 in W274 is unlikely to be of consequence.

Since the 5.3-kb and 3.9-kb RNAs contained common viral and *myb* sequences, we reasoned that the smaller species might be derived from the larger by a further splicing event. Because a transcript extending from the normal Mo-MLV cap site to the cryptic splice donor at position 1596 (SD_c in Fig. 8A) would retain the normal viral splice donor site at position 206 (SD_e in Fig. 8A), a splice from this site to a cryptic acceptor site within the viral sequences could generate the smaller RNA species. Inspection of the Mo-MLV *gag* sequence revealed a number of potential (29) splice acceptor sites; a few candidates were selected that would maximize the size of the intron (i.e., to account for the size difference between the major tumor-specific RNAs) while retaining a potential initiation codon at position 1513 (see Discussion). Oligonucleotides spanning the predicted splice junctions were again used as hybridization probes. One of these, SO1 (Fig. 8A), which contained Mo-MLV

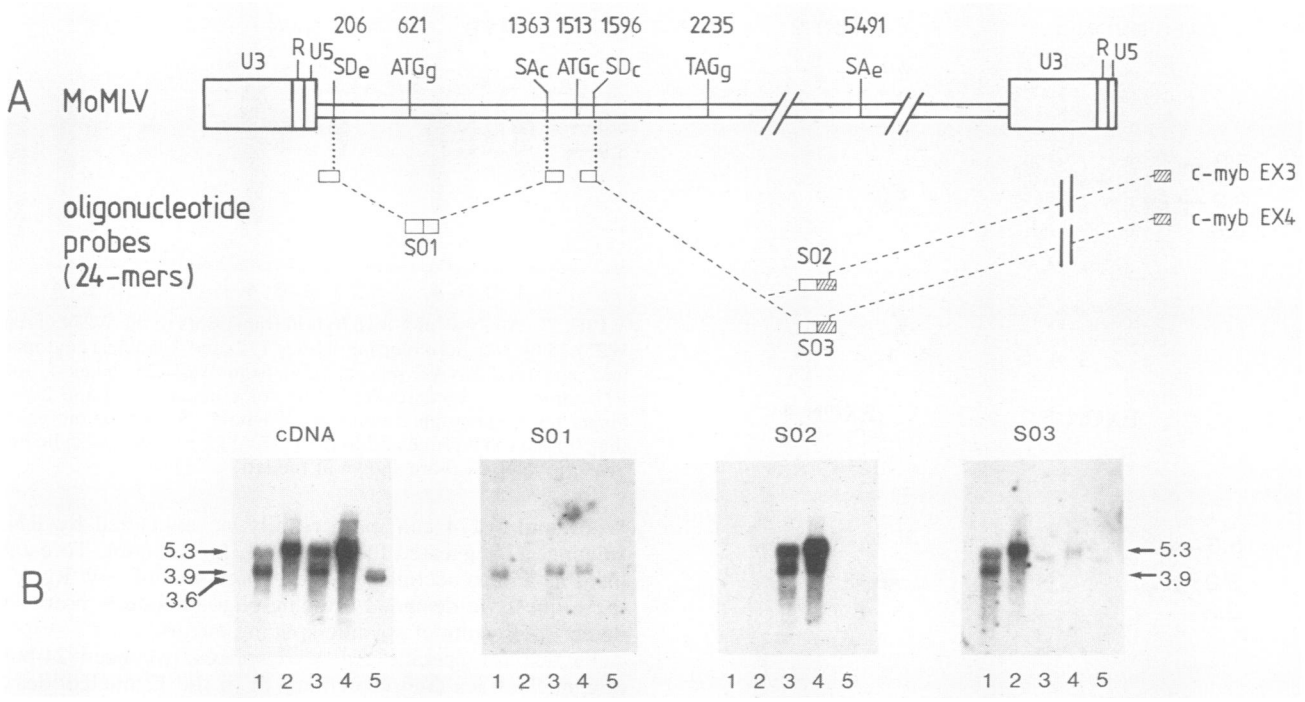

FIG. 8. Identification of splicing patterns of the abberrant viral-c-*myc* transcripts in W265 and W274. (A) The top of the figure represents the Mo-MLV proviral genome and shows the positions of splice donor (SD) and splice acceptor (SA) sites. Also shown are the relevant initiation (ATG) and termination (TAG) codons. Subscripts e, g, and c refer to envelope, *gag*, and cryptic, respectively. Numbers are nucleotide positions from the sequence of Shinnick et al. (47). Beneath the Mo-MLV map, the sequences represented in the bridging oligonucleotide probes SO1, SO2, and SO3 are illustrated (not to scale); hatched boxes represent sequences from the 5′ boundaries of the indicated c-*myb* exons (see text and Materials and Methods). (B) Northern blotting analyses of W265 and W274 RNAs with these probes and, for comparison, a c-*myb* cDNA probe. Lanes: 1, cytoplasmic RNA from W265; 2, nuclear RNA from W265; 3, cytoplasmic RNA from W274; 4, nuclear RNA from W274; 5, cytoplasmic RNA from RB22.

nucleotides 195 to 206 and 1362 to 1373, did in fact hybridize to the 3.9-kb RNAs of both W265 and W274 (Fig. 8B) but not to the 5.3-kb species, the Mo-MLV RNAs, or the normal c-*myb* transcript. Hence, we conclude that in both cell lines, the 3.9-kb species is generated from a 5.3-kb nuclear precursor by a splice from the normal envelope splice donor site (SD_e) to a cryptic splice acceptor site (SA_c) that removes 1,156 nucleotides of viral sequences.

DISCUSSION

We have shown here that the murine myeloid tumor lines W265 and W274 but not 15 other myeloid cell lines examined carry a rearranged c-*myb* gene (Table 1). In both cases Mo-MLV proviral sequences have inserted within the 5′ portion of the c-*myb* gene and have induced high levels of abnormal c-*myb* transcripts which contain viral sequences and lack sequences from the 5′ end of c-*myb*. Thus, as well as inducing transcriptional deregulation, the viral insertion has generated *myb* RNAs that lack sequences encoding the amino terminus of the c-*myb* protein. This truncation probably contributes to the oncogenicity of *myb* in these tumors, as suggested previously (15, 45).

These results are very similar to those obtained by Shen-Ong and co-workers with the ABPL tumors (30, 45, 46). Those tumors are now assigned to the myeloid lineage and, like W265 and W274, were induced in vivo by infection with Ab-MLV. Our analysis of the *myb* RNAs in W265 and W274 extends their findings by identifying the RNA that probably encodes the truncated *myb* protein and by demonstrating that the W274 RNAs contain c-*myb* sequences additional to those present in v-*myb*, W265, and the ABPL tumors.

Our RNA analysis was carried out with a combination of Northern blotting, subcellular fractionation, and specific oligonucleotide probes to identify and characterize the various *myb* RNAs in W265 and W274, since these techniques complement and extend data obtained by others (45) with cDNA cloning and S1 nuclease mapping. In particular, our approach allows the assignment of specific sequences to each RNA species detected and (in contrast to analysis of a single cDNA clone) can demonstrate that RNAs bearing these sequences are present at significant levels in the cells.

Generation and translational potential of *myb* RNAs in W265 and W274. Both W265 and W274 contain a high level of a predominantly nuclear 5.3-kb *myb* RNA and lower amounts of a predominantly cytoplasmic 3.9-kb species. Our finding that the latter RNA is generated from the former by a further splicing event may explain the subcellular distribution and relative abundance of these two species. That is, the presence of unused splicing sites, i.e., an intron, within the 5.3-kb RNA may cause it to be treated as a pre-mRNA and retained in the nucleus. Although retroviral genomic RNA can clearly reach the cytoplasm without splicing, the 5.3-kb *myb* RNA is a hybrid viral-cellular species and may not be processed and transported in the same way as authentic viral transcripts. Alternatively, it is possible that the 5.3-kb RNA retains some c-*myb* intron sequences and that these are responsible for its retention in the nucleus. In any case, the inefficiency of this unusual splicing step may reflect the fact that the acceptor site at position 1362 (SA_c in Fig. 8A) is not normally utilized. Indeed, it may only be used in this instance because the normal *env* acceptor site (SA_e in Fig. 8A) is probably absent from the deleted Mo-MLV proviruses

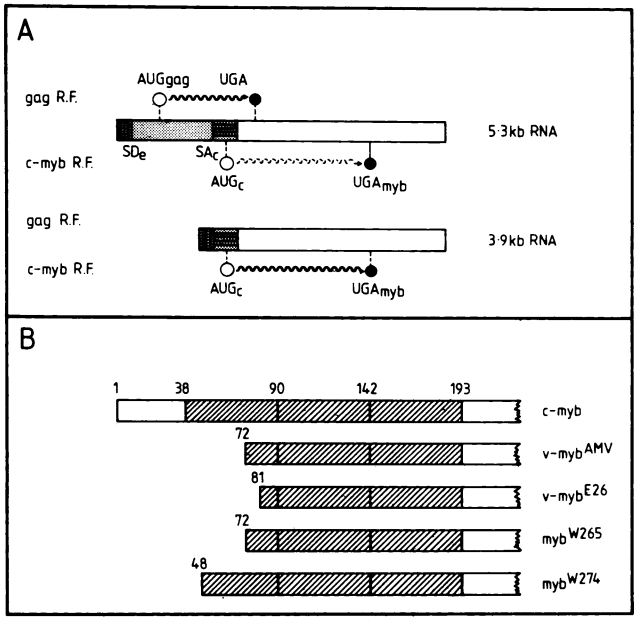

FIG. 9. (A) Model for the origin and translational potential of the viral-cellular hybrid RNAs of W265 and W274. The boxes represent the two major RNAs described in the text; stippled portions indicate viral sequences, while open portions indicate c-*myb* sequences. Wavy lines indicate the proteins encoded in the major open reading frames (R.F.); the corresponding initiation (AUG) and termination (UGA) codons are also shown. Also indicated on the 5.3-kb RNA are the splice sites (SD_c and SA_c, see Fig. 8) involved in the generation of the smaller species. For further explanation, see the text. (B) Relationship between predicted amino-terminal regions of *myb*-encoded proteins. The three hatched sections of each box represent the three 51- to 52-amino-acid repeats of the c-*myb* protein; amino acid numbers are those of the murine c-*myb* protein sequence.

in this class of tumors (46). The presence of cryptic splice sites within the Mo-MLV *gag* gene may also have implications for normal viral function, since the RNAs produced by infrequent splicing at these (or other) sites could give rise to previously unidentified viral gene products.

The observation that the major *myb* RNA species in W265 and W274, the 5.3-kb species, is predominantly if not exclusively nuclear implies that it may not be an mRNA. Indeed, even if some of this RNA were present in the cytoplasm, its translation is unlikely to yield a *myb* protein. Shen-Ong et al. (45) suggested that translation initiates with the AUG codon at Mo-MLV position 1513 (AUG_c in Fig. 9A). However, in a transcript retaining all viral sequences 5′ to the cryptic splice donor site (SD_c in Fig. 8A), the 5′-most AUG, at which translation of most eucaryotic mRNAs starts, would be that used to initiate translation of the *gag* gene product (47) (AUG_{gag} in Fig. 9A). Moreover, the *gag* reading frame is out of phase with that of *myb* and would terminate within the *myb* sequence downstream from AUG_c (Fig. 9A), further reducing the likelihood of initiation at that codon.

On the other hand, the splice demonstrated here between the normal viral donor site (SD_c) and the cryptic acceptor (SA_c) removes the normal *gag* initiation codon and much of the remaining *gag* sequence from the 5.3-kb RNA (Fig. 9A). Thus, the 3.9-kb *myb* RNA possesses only one major open reading frame, starting at the AUG at position 1513 (AUG_c; Fig. 9A). For this reason, and because of the predominantly cytoplasmic location of the 3.9-kb RNA, we propose that it is this mRNA which encodes the transforming *myb* proteins in W265 and W274 and probably also in the ABPL tumors.

Implications for transformation by *myb*. The *myb* proteins of AMV, E26, and the ABPL tumors are truncated at or near the boundary of the region encoded by c-*myb* exon 4 (19, 24, 31, 41, 45) and therefore lack about two-thirds of the first of three highly conserved 51 to 52-amino-acid tandem repeats (15) that lie near the amino terminus of the c-*myb* protein (Fig. 9B). Our data imply that the predicted *myb* protein in W265 is similarly truncated at the exon 4 boundary. However, the *myb* RNAs of W274 also contain the exon 3 sequence, and therefore the *myb* protein in W274 should contain all but 10 amino acids of the first repeat (Fig. 9B) (since the exon 3 boundary corresponds to residue 48 of the c-*myb* protein [15, 24; unpublished data]). Thus, it appears that truncation of the c-*myb* protein further toward the amino terminus may also activate its oncogenic potential, i.e., that there is no special significance to truncation precisely at the exon 4 boundary. Rather, activation may simply require disruption of the tandem repeat structure or, alternatively, loss of (all or part of) the 38-amino-acid sequence that precedes the repeats. Other structural alterations, such as the carboxy-terminal truncation predicted for the products of the rearranged c-*myb* gene in the NFS-60 cell line (45, 53) and of the v-*myb* genes (19, 31, 41) may also activate c-*myb*.

Our results also bear on the quantitative requirements for transformation by *myb*. The level of the 3.9-kb mRNA in W265 is similar to that of the normal 3.6-kb c-*myb* RNA in cells such as the thymoma cell line RB22 (e.g., Fig. 5), the myelomonocytic leukemia WEHI-3B, and normal myeloid progenitor cells (T.J.G., unpublished observations), suggesting that an abnormally high level of *myb* expression is not necessary for transformation. Similarly, Duprey and Boettiger (11) have noted that the level of c-*myb* RNA in a highly enriched population of chicken myeloid progenitor cells is similar to that of v-*myb* RNA in chicken "myeloblasts" transformed by E26.

In contrast to a number of other myeloid cell lines (Table 1) (54), the normal c-*myb* genes of W265 and W274 are expressed at low levels (or not at all), as also noted by Lavu and Reddy (24) for the ABPL2 tumor. This may reflect the differentiation state of the target cells for transformation by *myb*: for example, neither normal chicken macrophages nor macrophages transformed by AMV express the c-*myb* gene (16, 20). Alternatively, the low level of normal c-*myb* transcripts may reflect repression of the c-*myb* gene by the *myb* product itself, as has previously been suggested for c-*myc* (25).

Finally, the presence of an activated *myb* gene in W274 has interesting implications for oncogene cooperativity in the transformation of myeloid cells. While evidence for cooperativity between oncogenes in the transformation of fibroblasts and hematopoietic cells (17, 18, 22, 36, 44) is accumulating, it remains unclear which genes can augment the oncogenicity of *myb*. Therefore, it is probably pertinent that W274 also bears an activated Ha-*ras* gene (49), particularly since cooperativity between v-*myb* and *ras* in transforming primary fibroblasts has been mentioned in one report (33). Other oncogenes that may cooperate with *myb* could be involved in releasing the cells from dependence on colony-stimulating factors (CSFs), since cells transformed by v-*myb* (2) and truncated c-*myb* (53) genes remain CSF dependent. Release of hematopoietic cells from CSF dependence has been shown to induce or enhance tumorigenicity and can occur by a number of mechanisms, including

autocrine CSF production (17, 23, 43). Moreover, early-passage subclones of W274 that bear rearrangements of CSF genes and exhibit autocrine growth stimulation have recently been characterized (K. Leslie and J. Schrader, personal communication), suggesting that autocrine CSF production may indeed cooperate with *myb* in the malignant transformation of myeloid cells. Whether these subclones also possess activated *ras* genes is not known, but in any case these findings suggest that activation of *ras* and CSF genes may represent stages in the progression of myeloid leukemia induced by activation of c-*myb*.

ACKNOWLEDGMENTS

We thank Julie King and Ashley Dunn for isolating one of the c-*myb* genomic clones and Kevin Leslie and John Schrader for the W274.25 cell line and for permission to quote unpublished results. We are also grateful to Julie de Blaquiere, Leonie Gibson, and Lynda Byrt for excellent technical assistance and to Pierre Smith, Allan May, Sonya Belan, and Louise Ellis for assistance in preparing the manuscript. In addition, we thank Michael Eefting and Denis Scanlon of the Joint Protein Structure Laboratory of the Ludwig Institute and Walter and Eliza Hall Institute for preparation of synthetic oligonucleotides.

This work was supported in part by grants to S.C. and J.M.A. from the National Health and Medical Research Council (Canberra), the National Cancer Institute (Public Health Service grant CA-12421), the American Heart Foundation, and the Drakensberg Trust.

LITERATURE CITED

1. **Bender, T. P., and W. M. Kuehl.** 1986. Murine *myb* proto-oncogene mRNA: cDNA sequence and evidence for 5′ heterogeneity. Proc. Natl. Acad. Sci. USA **83**:3204–3208.
2. **Beug, H., M. J. Hayman, and T. Graf.** 1982. Myeloblasts transformed by the avian acute leukemia virus E26 are hormone-dependent for growth and for the expression of a putative *myb*-containing protein, p135 E26. EMBO J. **1**:1069–1073.
3. **Beug, H., A. von Kirchbach, G. Doderlein, J.-F. Conscience, and T. Graf.** 1979. Chicken hematopoietic cells transformed by seven strains of defective avian leukemia viruses display three distinct phenotypes of differentiation. Cell **18**:375–390.
4. **Castle, S., and D. Sheiness.** 1985. Structural organization of the mouse proto-myb gene. Biochem. Biophys. Res. Commun. **132**:688–695.
5. **Cook, W. D.** 1985. Thymocyte subsets transformed by Abelson murine leukemia virus. Mol. Cell. Biol. **5**:390–397.
6. **Cory, S., S. Gerondakis, and J. M. Adams.** 1983. Interchromosomal recombination of the cellular oncogene *c-myb* with the immunoglobulin heavy chain locus in murine plasmacytomas is a reciprocal exchange. EMBO J. **2**:697–703.
7. **Daube, S. K., I. B. Pragnell, N. Kluge, G. Gaedicke, G. Steinheider, and W. Ostertag.** 1975. Induction of endogenous and of spleen focus-forming viruses during dimethylsulfoxide-induced differentiation of mouse erythroleukemia cells transformed by spleen focus-forming virus. Proc. Natl. Acad. Sci. USA **72**:1863–1867.
8. **Dexter, T. M., T. D. Allen, D. Scott, and N. M. Teich.** 1979. Isolation and characterization of bipotential haematopoietic cell line. Nature (London) **277**:471–474.
9. **Dexter, T. M., J. Garland, D. Scott, E. Scolnick, and D. Metcalf.** 1980. Growth of factor-dependent hemopoietic precursor cell lines. J. Exp. Med. **152**:1036–1047.
10. **Dozier, C., M. S. Walbaum, D. Leprince, and D. Stehelin.** 1986. EcoRI RFLP linked to human *myb* gene. Nucleic Acids Res. **14**:1928.
11. **Duprey, S. P., and D. Boettiger.** 1985. Developmental regulation of *c-myb* in normal myeloid progenitor cells. Proc. Natl. Acad. Sci. USA **82**:6937–6941.
12. **Favaloro, J. R., R. Treisman, and R. Kamen.** 1980. Transcription maps of polyoma virus-specific RNA: analysis by two-dimensional nuclease S1, gel mapping. Methods Enzymol. **65**:718–749.
13. **Furth, J., P. Hagen, and E. J. Hirsch.** 1957. Transplantable mastocytoma in the mouse containing histamine, heparin and 5-hydroxytryptamine. Proc. Soc. Exp. Biol. Med. **95**:824–828.
14. **Gerondakis, S., and J. M. Bishop.** 1986. Structure of the protein encoded by the chicken proto-oncogene c-*myb*. Mol. Cell. Biol. **6**:3677–3684.
15. **Gonda, T. J., N. M. Gough, A. R. Dunn, and J. de Blaquiere.** 1985. Nucleotide sequence of cDNA clones of the murine *myb* proto-oncogene. EMBO J **4**:2003–2008.
16. **Gonda, T. J., D. K. Sheiness, and J. M. Bishop.** 1982. Transcripts from the cellular homologs of retroviral oncogenes: distribution among chicken tissues. Mol. Cell. Biol. **2**:617–624.
17. **Graf, T., F. von Weizsaecker, S. Grieser, J. Coll, D. Stehelin, T. Patschinsky, K. Bister, C. Bechade, G. Calothy, and A. Leutz.** 1986. *v-mil* induces autocrine growth and enhanced tumorigenicity in *v-myc*-transformed avian macrophages. Cell **45**:357–364.
18. **Kahn, P., L. Frykberg, C. Brady, I. Stanley, H. Beug, B. Vennstrom, and T. Graf.** 1986. v-erbA cooperates with sacroma oncogenes in leukemic cell transformation. Cell **45**:349–356.
19. **Klempnauer, K.-H., T. J. Gonda, and J. M. Bishop.** 1982. Nucleotide sequence of the retroviral leukemia gene *v-myb* and its cellular progenitor *c-myb*: the architecture of a transduced oncogene. Cell **31**:453–463.
20. **Klempnauer, K-H., G. Ramsay, J. M. Bishop, M. G. Moscovici, C. Moscovici, J. P. McGrath, and A. D. Levinson.** 1983. The product of the retroviral transforming gene *v-myb* is a truncated version of the protein encoded by the cellular oncogene *c-myb*. Cell **33**:345–355.
21. **Koren, H. S., B. S. Handwerger, and J. R. Wunderlich.** 1975. Identification of macrophage-like characteristics in a cultured murine tumor line. J. Immunol. **114**:894–897.
22. **Land, H., L. F. Parada, and R. A. Weinberg.** 1983. Cellular oncogenes and multistep carcinogenesis. Science **222**:771–778.
23. **Lang, R. A., D. Metcalf, N. M. Gough, A. R. Dunn, and T. J. Gonda.** 1985. Expression of a hemopoietic growth factor cDNA in a factor-dependent cell line results in autonomous growth and tumorigenicity. Cell **43**:531–542.
24. **Lavu, S., and E. P. Reddy.** 1986. Structural organization and nucleotide sequence of mouse *c-myb* oncogene: activation in ABPL tumors is due to viral integration in an intron which results in the deletion of the 5′ coding sequences. Nucleic Acids Res. **14**:5309–5320.
25. **Leder, P., J. Battey, G. Lenoir, C. Moudling, W. Murphy, H. Potter, T. Stewart, and R. Taub.** 1983. Translocations among antibody genes in human cancer. Science **222**:765–771.
26. **Maniatis, T., E. F. Fritsch, and J. Sambrook.** 1982. Molecular cloning: a laboratory manual. Cold Spring Harbor Laboratory, Cold Spring Harbor, N.Y.
27. **Meinkoth, J., and G. Wahl.** 1984. Hybridization of nucleic acids immobilized on solid supports. Anal. Biochem. **138**:267–284.
28. **Moscovici, C.** 1975. Leukemic transformation with avian myeloblastosis virus: present status. Curr. Top. Microbiol. Immunol. **71**:79–101.
29. **Mount, S. M.** 1982. A catalogue of splice function sequences. Nucleic Acids Res. **10**:459–472.
30. **Mushinski, J. F., M. Potter, S. R. Bauer, and E. P. Reddy.** 1983. DNA rearrangement and altered RNA expression of the *c-myb* oncogene in mouse plasmacytoid lymphosarcomas. Science **220**:795–798.
31. **Nunn, M. F., P. H. Seeburg, C. Moscivici, and P. H. Duesberg.** 1983. Tripartite structure of the avian erythroblastosis virus E26 transforming gene. Nature (London) **306**:391–395.
32. **Nusse, R.** 1986. The activation of cellular oncogenes by retroviral insertion. Trends Genet. **2**:244–247.
33. **Parada, L. F., H. Land, R. A. Weinberg, D. Wolf, and V. Rotter.** 1984. Cooperation between gene encoding p53 tumour antigen and *ras* in cellular transformation. Nature (London) **312**:649–651.
34. **Ralph, P., M. A. S. Moore, and K. Nilsson.** 1976. Lysozyme synthesis by established human and murine histiocytic lym-

phoma cell lines. J. Exp. Med. **143**:1528–1533.
35. **Ralph, P., J. Prichard, and M. Cohn.** 1975. Reticulum cell sarcoma: an effector cell in antibody-dependent cell-mediated immunity. J. Immunol. **114**:898–905.
36. **Rapp, U. R., J. L. Cleveland, T. N. Fredrickson, K. L. Holmes, H. C. Morse III, H. W. Jansen, T. Patschinsky, and K. Bister.** 1985. Rapid induction of hemopoietic neoplasms in newborn mice by a *raf(mil)/myc* recombinant murine retrovirus. J. Virol. **55**:23–33.
37. **Raschke, W. C., S. Baird, D. Ralph, and I. Nakoinz.** 1978. Functional macrophage cell line transformed by Abelson leukemia virus. Cell **15**:261–267.
38. **Reddy, E. P., M. J. Smith, and A. Srinivasan.** 1983. Nucleotide sequence of Abelson murine leukemia virus genome: structural similarity of its transforming gene product to other onc gene products with tyrosine-specific kinase activity. Proc. Natl. Acad. Sci. USA **80**:3623–3627.
39. **Rosson, D., and E. P. Reddy.** 1986. Nucleotide sequence of chicken *c-myb* complementary DNA and implications for myb oncogene activation. Nature (London) **319**:604–606.
40. **Roussel, M., S. Saule, C. Lagrou, C. Rommens, H. Beug, T. Graf, and D. Stehelin.** 1979. Three new types of viral oncogene of cellular origin specific for haematopoietic cell transformation. Nature (London) **281**:452–455.
41. **Rushlow, K. E., J. A. Lautenberger, T. S. Papas, M. A. Baluda, B. Perbal, J. G. Chirikjian, and E. P. Reddy.** 1982. Nucleotide sequence of the transforming gene of avian myeloblastosis virus. Science **216**:1421–1423.
42. **Schindler, R., M. Day, and G. A. Fischer.** 1957. Culture of neoplastic mast cells and their synthesis of 5-hydroxytryptamine and histamine *in vitro*. Cancer Res. **19**:47–51.
43. **Schrader, J. W., and R. M. Crapper.** 1983. Autogenous production of a hemopoietic growth factor, persisting-cell-stimulating factor, as a mechanism for transformation of bone marrow-derived cells. Proc. Natl. Acad. Sci. USA **80**:6892–6896.
44. **Schwartz, R. C., L. W. Stanton, R. C. Riley, K. B. Marcu, and O. N. Witte.** 1986. Synergism of v-*myc* and v-Ha-*ras* in the in vitro neoplastic progression of murine lymphoid cells. Mol. Cell. Biol. **6**:3221–3231.
45. **Shen-Ong, G. L. C., H. C. Morse III, M. Potter, and S. Mushinski.** 1986. Two modes of c-*myb* activation in virus-induced mouse myeloid tumors. Mol. Cell. Biol. **6**:380–392.
46. **Shen-Ong, G. L. C., M. Potter, J. F. Mushinski, S. Lavu, and E. P. Reddy.** 1984. Activation of the *c-myb* locus by viral insertional mutagenesis in plasmacytoid lymphosarcomas. Science **226**:1077–1080.
47. **Shinnick, T. M., R. A. Lerner, and J. G. Sutcliffe.** 1981. Nucleotide sequence of Moloney murine leukaemia virus. Nature (London) **293**:543–548.
48. **Srinivasan, A., E. P. Reddy, and S. A. Aaronson.** 1981. Abelson murine leukemia virus: molecular cloning of infectious integrated proviral DNA. Proc. Natl. Acad. Sci. USA **78**:2077–2081.
49. **Vousden, K. H., and C. J. Marshall.** 1984. Three different activated ras genes in mouse tumours: evidence for oncogene activation during progression of a mouse lymphoma. EMBO J. **3**:913–917.
50. **Warner, N. L., S. W. Burchiel, and E. B. Walker.** 1979. Characterization of murine B cell lymphomas and macrophage tumors by flow microfluorometry and functional assays, p. 243–261. *In* W. D. Terry and Y. Yamamura (ed.), Immunobiology and immunotherapy of cancer. Elsevier/North-Holland, Amsterdam.
51. **Warner, N. L., R. K. Cheney, L. L. Lanier, M. Daley, and E. Walker.** 1982. Differentiation heterogeneity in murine hematopoietic tumors, p. 223–243. *In* M. A. S. Moore (ed.), Maturation factors and cancer. Raven Press, New York.
52. **Warner, N. L., M. A. S. Moore, and D. Metcalf.** 1969. A transplantable myelomonocytic leukemia in BALB/c mice: cytology, karyotype, and muramidase content. J. Natl. Cancer Inst. **43**:963–982.
53. **Weinstein, Y., J. N. Ihle, S. Lavu, and E. P. Reddy.** 1986. Truncation of the *c-myb* gene by a retroviral integration in an interleukin 3-dependent myeloid leukemia cell line. Proc. Natl. Acad. Sci. USA **83**:5010–5014.
54. **Westin, E. H., R. C. Gallo, S. K. Arya, A. Eva, L. M. Souza, M. A. Baluda, S. A. Aaronson, and F. Wong-Staal.** 1982. Differential expression of the amv gene in human hematopoietic cells. Proc. Natl. Acad. Sci. USA **79**:2194–2198.